



## Original Article

## The subsequent biological effects of simulated microgravity on endothelial cell growth in HUVECs

Dan Xu <sup>a</sup>, Yu-Bing Guo <sup>a</sup>, Min Zhang <sup>a, b</sup>, Ye-Qing Sun <sup>a, \*</sup><sup>a</sup> Institute of Environmental Systems Biology, Dalian Maritime University, Dalian 116026, China<sup>b</sup> Department of Molecular Physiology and Medical Bioregulation, Yamaguchi University, 1-1-1 Minami-Kogushi, Ube, 755-8505, Japan

## ARTICLE INFO

## Article history:

Received 1 November 2017

Received in revised form

17 February 2018

Accepted 28 February 2018

Available online 28 June 2018

## Keywords:

Simulated microgravity

Growth inhibition

miR-22

Serum response factor

LAMC1

mTOR

## ABSTRACT

**Purpose:** Microgravity is known to cause endothelium dysfunction in astronauts returning from spaceflight. We aimed to reveal the regulatory mechanism in alterations of human endothelial cells after simulated microgravity (SMG).

**Methods:** We utilized the rotary cell culture system (RCCS-1) to explore the subsequent effects of SMG on human umbilical vein endothelial cells (HUVECs).

**Results:** SMG-treated HUVECs appeared obvious growth inhibition after return to normal gravity, which might be attributed to a set of responses including alteration of cytoskeleton, decreased cell adhesion capacity and increased apoptosis. Expression levels of mTOR and its downstream Apaf-1 were increased during subsequent culturing after SMG. miR-22 was up-regulated and its target genes SRF and LAMC1 were down-regulated at mRNA levels. LAMC1 siRNAs reduced cell adhesion rate and inhibited stress fiber formation while SRF siRNAs caused apoptosis.

**Conclusion:** SMG has the subsequent biological effects on HUVECs, resulting in growth inhibition through mTOR signaling and miR-22-mediated mechanism.

© 2018 Chinese Medical Association. Production and hosting by Elsevier B.V. This is an open access article under the CC BY-NC-ND licence (<http://creativecommons.org/licenses/by-nc-nd/4.0/>).

## Introduction

Space environment is characterized by high LET radiation, ultra-high vacuum, weak magnetic field and microgravity. Spaceflight may cause skeletal muscle atrophy, bone loss and dysfunction of cardiovascular systems, which are due to the effects of microgravity.<sup>1,2</sup> Ground-based simulated microgravity (SMG) conditions can be achieved through the use of the most advanced rotary cell culture system (RCCS-1). The rotational motion of this system prevents sedimentation by randomization of the gravity vector, creating an optimized suspension culture capable of supporting 3-D cell growth on micro-carrier bead scaffolds.<sup>3</sup> Thus, RCCS-1 can effectively simulate certain aspects of microgravity, which is helpful for better understanding of the effects of microgravity on many cellular activities.

Studies have revealed that microgravity can exert its detrimental effects on astronauts via changes in cellular structure

and/or functions. Recently, there has been more research interest in the effect of microgravity on the structure and function of human cells. Cytoskeletal disruption occurs in several cell types including lymphocytes, glial cells, and osteoblasts both during spaceflight and in SMG.<sup>4–6</sup> It is reported that phenotypic switch was induced by SMG on human breast cancer MDA-MB-231 cells, characterized by different morphologies.<sup>7</sup> SMG induced partial arrest in G2/M phase in MCF-7 cells<sup>8</sup> and inhibited cell growth in malignant glioma cells due to a slowdown of the processions of all the cell cycle phases.<sup>9</sup>

Endothelium is one of the tissues most sensitive to microgravity conditions. Endothelial cells form the inner lining of blood vessels and provide a semi-permeable barrier between the blood and underlying tissues, thus playing an important role in the maintenance of the vascular homeostasis.<sup>10</sup> Endothelial cells are highly sensitive to mechanical stress, including hypergravity and microgravity. They undergo morphological and functional changes in response to alterations of gravity.<sup>11,12</sup> In particular microgravity leads to changes in endothelial cell phenotype and behavior.<sup>13–15</sup> Endothelial dysfunction is regarded as an early event in atherosclerosis, possibly associated with vascular alterations of cardiovascular system disorders in spaceflight and post-

\* Corresponding author.

E-mail address: [yqsun@dlmu.edu.cn](mailto:yqsun@dlmu.edu.cn) (Y.-Q. Sun).

Peer review under responsibility of Daping Hospital and the Research Institute of Surgery of the Third Military Medical University.

flight period. At the end of the 12-day outer spaceflight, it is reported that endothelial cells displayed profound changes including cytoskeletal disruption, premature senescence, and increased cell membrane permeability. Readapted cells of subsequent passages exhibited persisting cytoskeletal changes, decreased metabolism and cell growth indicating endothelial dysfunction.<sup>16</sup> However, there are very few studies on the mechanisms in the functional alteration of human endothelial cells during subsequent culturing after SMG treatment.

Serum Response Factor (SRF) is a serum response element-binding transcription factor, which encodes a ubiquitous nuclear protein that participates in cell cycle regulation, cell proliferation and apoptosis. It is reported that SRF is a key regulator for endothelial cell function and plays important roles in multiple aspects of atherogenesis. Downregulation of SRF inhibited cell proliferation and induced apoptosis of endothelial cells, which contributed to endothelial dysfunction.<sup>17</sup> The target of rapamycin (TOR) is a highly conserved protein kinase and a central controller of cell growth. Mammalian target of rapamycin (mTOR) is a critical regulator in vascular endothelial cells responding to upstream cellular signals, such as growth factors and stress, participating in controlling cell proliferation, apoptosis, protein synthesis and metabolism.<sup>18</sup> It is reported that Phosphatase and Tensin Homolog (PTEN) could suppress mTOR expression by acting as an upstream regulator of mTOR, promoting apoptosis.<sup>19</sup> Apoptotic protease activating factor-1 (Apaf-1), one of pro-apoptotic proteins, functions in downstream apoptotic pathway of mTOR signaling.<sup>20</sup> mTOR may be involved in the development of atherosclerotic plaque, and dysregulation of mTOR signaling often occurs in human cardiovascular diseases.<sup>21</sup> Laminin family assemble from  $\alpha$ -,  $\beta$ - and  $\gamma$ -chain, which play a role in cell proliferation, adhesion, spreading and migration in both normal and pathologic processes.<sup>22</sup> The laminin  $\gamma$ -1 chain is the most ubiquitously expressed  $\gamma$  subunit, encoded by LAMC1 that can influence intracellular pathway to regulate the cytoskeleton changes and interfere endothelial barrier function.<sup>23</sup>

The aim of this study was to identify the exact cellular changes and epigenetic mechanism in alterations of human endothelial cells during subsequent culture after SMG treatment. We found that HUVECs exhibited remarkable growth inhibition, which might be attributed to a set of responses including alteration of cytoskeleton, decreased cell adhesion capacity and increased apoptosis. The mechanism of growth inhibition may be explained by the decrease in miR-22 targeting SRF and LAMC1 mRNAs, and the increase in the expression levels of Apaf-1 in mTOR signaling. This study provides a better understanding of the underlying mechanisms in the dysfunction of the cardiovascular systems after microgravity.

## Methods

### Cell culture and SMG treatment

HUVECs cells were obtained from Shanghai Institutes for Biological Sciences, China. Cells were grown in RPMI 1640 medium (KeyGen, Nanjing, China) containing 10% fetal bovine serum (GIBCO) and 1% penicillin-streptomycin at 37 °C in a humidified incubator with 5% CO<sub>2</sub>. Hillex II microcarrier beads (Solohill Engineering Laboratories, MI) were used as described in previous report.<sup>24</sup> Briefly,  $1 \times 10^6$  cells were seeded onto 50 mg microcarrier beads in 60 mm petri dishes in normal culture condition for 24 h. This timeline was sufficient to allow HUVECs to attach to the microcarrier surface. Then, they were transferred to either 50-ml high aspect ratio vessels (HARVs) in the RCCS-1 (NASA, USA) to

model microgravity or to 60 mm petri dishes for gravity controls (G). The culture of cell-beads was performed in this device in a 5% CO<sub>2</sub> incubator at 95% humidity. The horizontally rotating culture vessel was filled with the complete medium (without air-liquid interface to reduce the shear stress). After a defined rotational speed was reached, the cells were maintained in a near laminar fluid flow environment (i.e., a free-fall state). To study subsequent effects of SMG, HUVECs in both the G and SMG groups were detached from microcarriers using 0.05% Trypsin and 0.02% EDTA, and then cultured in normal growth condition for the indicated time.

### Cell proliferation analysis

HUVECs were seeded in 35 mm culture dishes at a concentration of  $5 \times 10^4$  cells. Cells were stained with 0.4% trypan blue and viable cells were counted using a hemocytometer at several time-lines (24, 48, 72 and 96 h). For each sample, the experiments were performed in triplicates ( $n = 3$ ).

### Cell adhesion assay

HUVECs were seeded at a concentration of  $5 \times 10^5$  cells per 35 mm culture dish. At the indicated time points (2, 4 and 6 h), the cells adhere to the dish or the cells in the medium were collected separately and the cell number was estimated using a hemocytometer. The adhesion rate is the ratio of adhesive cells to the sum of adhesive cells and detached cells in the medium as described previously.<sup>25</sup>

### Immunofluorescence assay

HUVECs were washed with PBS, fixed with 4% paraformaldehyde, and permeabilized in 0.1% Triton X-100. Cells were blocked in 1% BSA, and incubated with anti-FAK antibody (1:200, Upstate), followed by goat anti-rabbit IgG antibody conjugated with Alexa Fluor 488 (1:500, Molecular Probes). F-actin was labeled with the Rhodamine-conjugated phalloidin (Invitrogen). After washing, cells were mounted with mounting medium (Vectashield) containing 0.25  $\mu$ g/ml DAPI and processed for immunofluorescence using a Leica fluorescence confocal microscope (Leica TCS Sp5 II, Germany) or an inverted fluorescence microscope (Nikon ECLIPSE TE2000-E, Japan). Images were acquired using a 60  $\times$  oil immersion objective. Fluorescence intensity of the cells was calculated by using image analysis module of Adobe Photoshop ver. 7.0. Actin stress fiber formation was quantified by counting the average number of stress fibers in at least five random independent fields under fluorescent confocal microscope as previously described.<sup>26</sup>

### Apoptosis assays

HUVECs were collected and stained with Annexin-V-FITC and PI according to the manufacturer's protocol of the Annexin V-FITC Apoptosis Detection Kit (KeyGen, Nanjing). The fluorescence intensity of cells was then evaluated by flow cytometry (BD Biosciences, CA) using quadrant statistics for apoptotic cell populations.

### Quantitative real-time PCR analysis

Total RNA was extracted from cells using TRIzol reagent (Invitrogen). The expression levels of miRNAs and mRNAs were quantified by TaqMan miRNA assays (Applied Biosystems) and SYBR

green (Invitrogen), respectively. Real-time PCR reactions were performed using ABI 7300 real-time PCR system (Applied Biosystems). PCR primers used were SRF sense, CGTTCA-CAGTCACCAACCTG and antisense, TGCCTGTACTCTTCAGACA; mTOR sense, CAGTTCGCCAGTGGACTGAAG, and antisense, GCTGGTCATAGAAGCGAGTAGAC; GAPDH sense, GAGTCAACG-GATTGGTCGT and antisense, TGGGATTCCATTGATGACA. The relative expression levels of miRNAs and mRNAs were calculated using the comparative delta CT method ( $2^{-\Delta\Delta CT}$ ) after normalization with reference to the expression of U6 small nuclear RNA and GAPDH, respectively.

*Luciferase reporter assay*

The 3'-UTR fragments of human LAMC1 (NM\_002293.3) containing three putative miR-22 binding sites or mutant sequence were cloned at the XhoI and NotI sites into the pmiR-RB-REPORT luciferase reporter vector (RiboBio Co. Ltd., Guangzhou, China). These constructs were named pmiR-LAMC1-WT and pmiR-LAMC1-Mut1 (deletion of seed region) or Mut2 (base substitution in seed region). All the constructs were further confirmed by sequencing. Each construct was cotransfected with miR-22 mimics or miR-NC (RiboBio) in a 96-well plate using Lipofectamine 2000 (Invitrogen) for 48 h. Luciferase activity was presented by relative hRlu/hluc ratio as previously described.<sup>27</sup>

*Transient siRNA transfection*

SRF or LAMC1 siRNAs (siRNA-1,2,3) and negative control siRNA (NC siRNA) were purchased from Biomics (Jiangsu, China). Cells were transfected with 10 nM of siRNA using LipofectamineRNAiMax (Invitrogen) according to the manufacturer's protocol.<sup>27</sup>

*Western blotting*

Cells were homogenised in lysis buffer [10-mM Tris-HCl (pH 7.4), 150-mM NaCl, 1% NP-40, 10-mM NaF, 0.2-mM Na<sub>3</sub>VO<sub>4</sub> and protease inhibitor (Sigma–Aldrich)]. Proteins (30 µg) were fractionated on 10% SDS-PAGE, blotted onto a polyvinylidene difluoride membrane (Millipore, MA) and probed with primary antibodies, including SRF, LAMC1 (Santa Cruz, CA) and Apaf-1 (Proteintech, Wuhan). GAPDH (ZSGQ-BIO, Beijing) was used as a loading control. The secondary antibodies were HRP-conjugated anti-rabbit (NA 934V) and anti-mouse (NA 931V) antibodies (GE Healthcare Life Sciences, MA). Proteins were visualised by chemiluminescence according to the manufacturer's instructions (Thermo, PA), followed by exposure to X-ray film. The density of bands was densitometrically quantified using ImageJ (National Institutes of Health, MD).

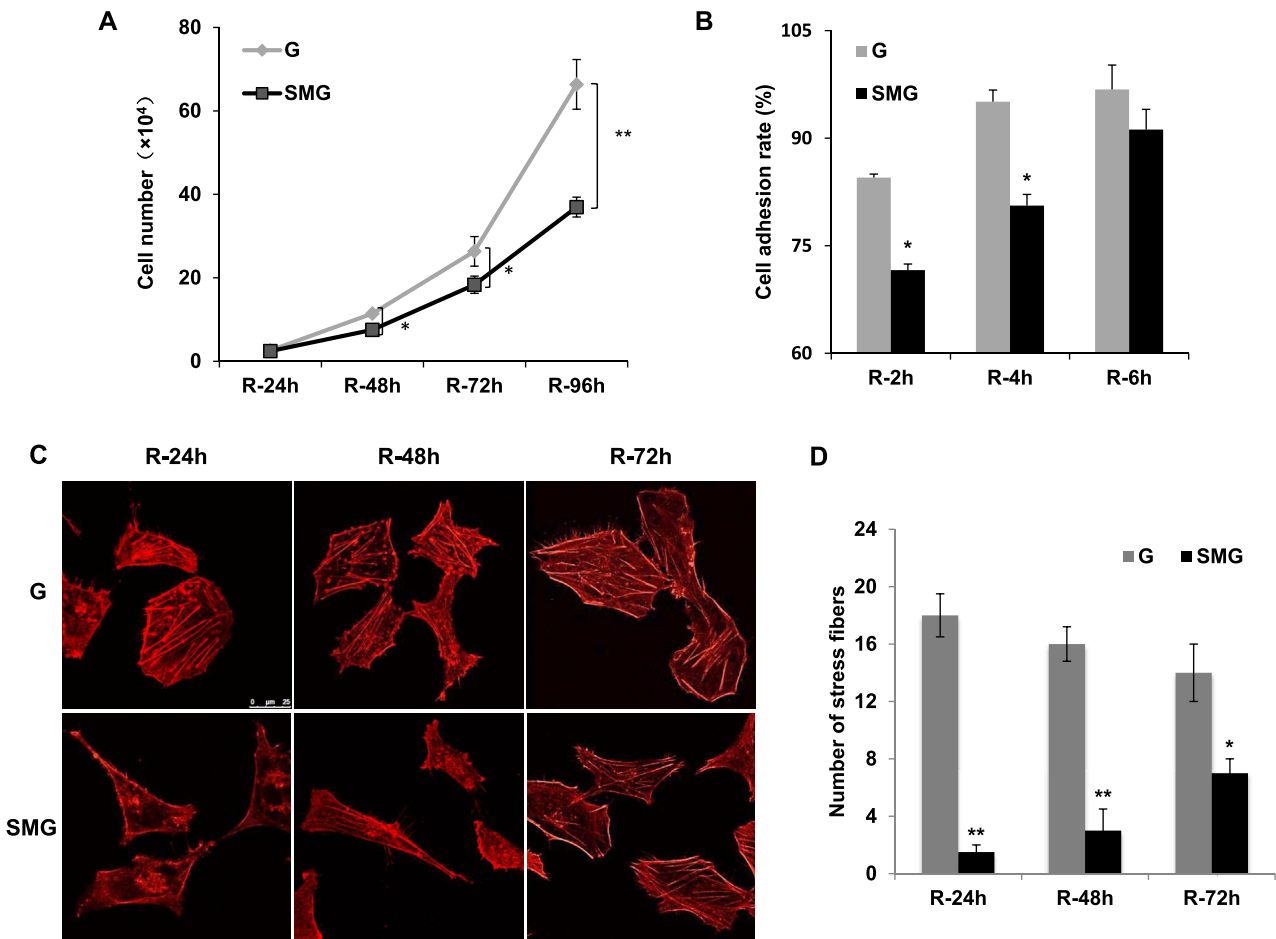


**Fig. 1.** Cellular changes during subsequent culturing after SMG treatment. A: Cell growth curve. B: Cell adhesion rate. C: Actin stress fibers were stained with the Rhodamine-conjugated phalloidin. Scale bar, 25 µm. D: Number of actin stress fibers was presented. \**p* < 0.05, \*\**p* < 0.01 vs G. Data was presented at indicated time points in the G and SMG groups after return to normal gravity. R indicates return to normal gravity.

### Statistical analysis

Experimental data for each variable were presented as mean  $\pm$  SD. The data were evaluated by Student's two-tail *t*-tests conducted in Microsoft Excel. \**p* < 0.05 means significant difference and \*\**p* < 0.01 implies great significant difference.

## Results

### Cellular changes during subsequent culturing after SMG treatment

To study subsequent effects of SMG, HUVECs were detached from the microcarrier beads and returned to normal growth conditions. We firstly examined cell growth rate by counting the cells at 24, 48, 72 and 96 h (Fig. 1A). There were significantly fewer cells in the SMG group compared to the G group after return to normal gravity (*p* < 0.05 after 48 and 72 h, *p* < 0.01 after 96 h).

It is known that cell adhesion is the process cells interact and attach to a surface, which is essential in maintaining cellular structure and promoting cell growth. We examined cell adhesion rate in earlier time after return to normal gravity and found the adhesion rates in the SMG group were significantly reduced at 2 h and 4 h of subculture (*p* < 0.05). At 6 h, only very slight reduced adhesion rates were observed in the SMG group (Fig. 1B).

We observed the alteration of actin cytoskeleton in the G group and SMG group at 24 h, 48 h and 72 h of subculture

(Fig. 1C). F-actin was labeled with phalloidin to analyze the number of stress fibers. Results showed that the formation of actin stress fibers remarkably reduced in SMG group compared to the G group at 24 h (*p* < 0.01), 48 h (*p* < 0.01) and 72 h (*p* < 0.05) after return to normal gravity (Fig. 1D).

### Apoptosis during subsequent culturing after SMG treatment

We performed apoptosis assays using flow cytometry in later time after return to normal gravity. Fig. 2A shows the representative results of apoptosis at 72 h and 96 h of subculture. The percentages of total apoptotic cells were significantly higher in the SMG Group than those in the G group (*p* < 0.05) after return to normal gravity (Fig. 2B). qRT-PCR results showed that the expression levels of mTOR mRNA were significantly up-regulated in SMG group compared to G group at 48 h, 72 h and 96 h (*p* < 0.01) of subculture after SMG (Fig. 2C). We also observed the remarkable increase in Apaf-1 protein level in downstream apoptotic pathway of mTOR signaling at 72 h and 96 h of subculture after SMG (Fig. 2D).

### Involvement of miR-22 in cellular changes during subsequent culturing after SMG treatment

We previously reported that miR-22 is one of critical regulators for vascular endothelial cell function.<sup>27</sup> qRT-PCR results

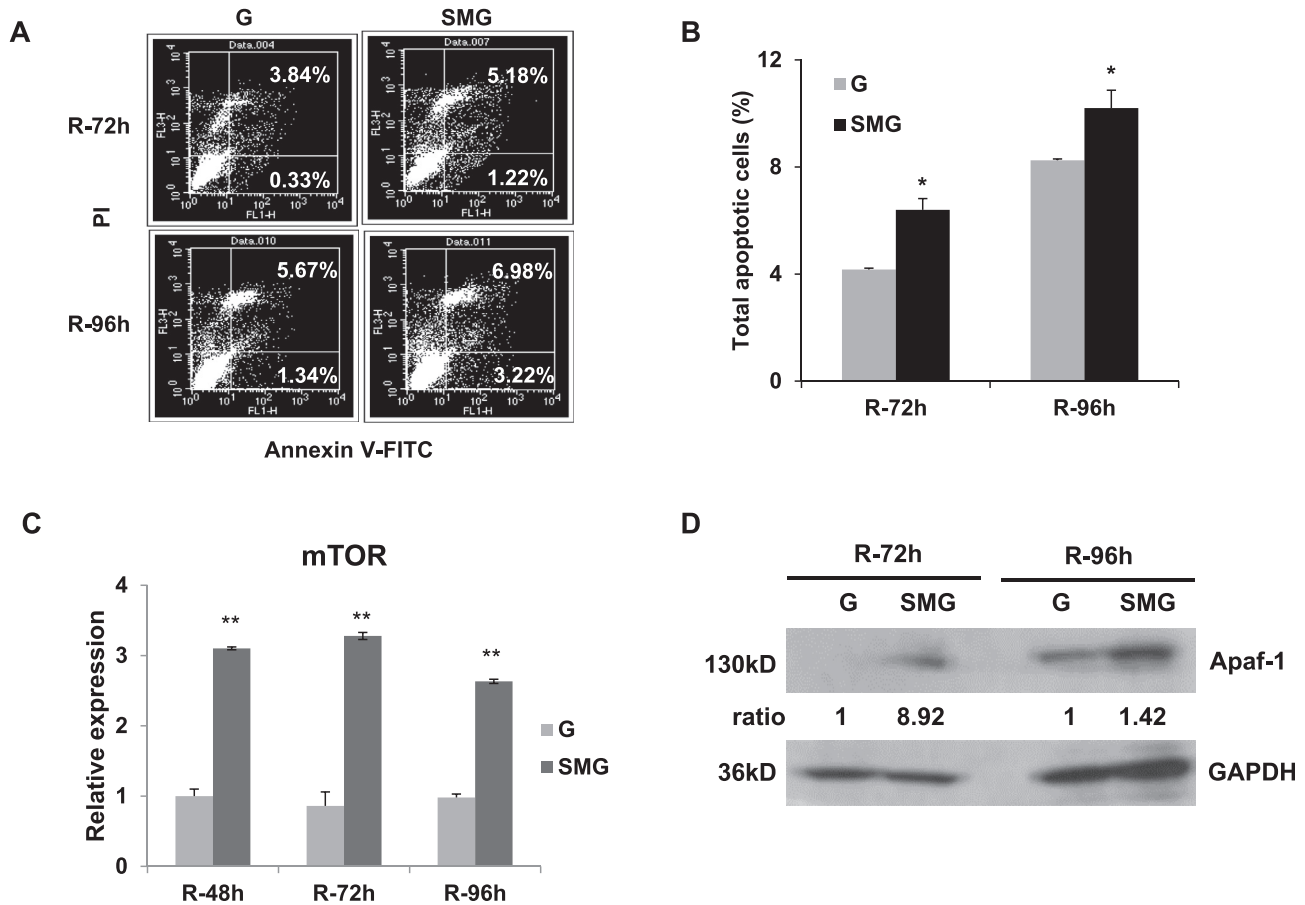


**Fig. 2.** The subsequent effect of SMG on apoptosis of HUVECs. Flow cytometry analysis was performed as described in Materials and methods. A: Early and later apoptotic rates were shown in representative histograms. B: Percentage of total apoptotic cells was presented in different groups. C: The relative expression level of mTOR mRNA was quantified by qRT-PCR analysis. D: Apaf-1 protein was examined by western blot analysis. \**p* < 0.05. \*\**p* < 0.01 vs G. R indicates return to normal gravity.

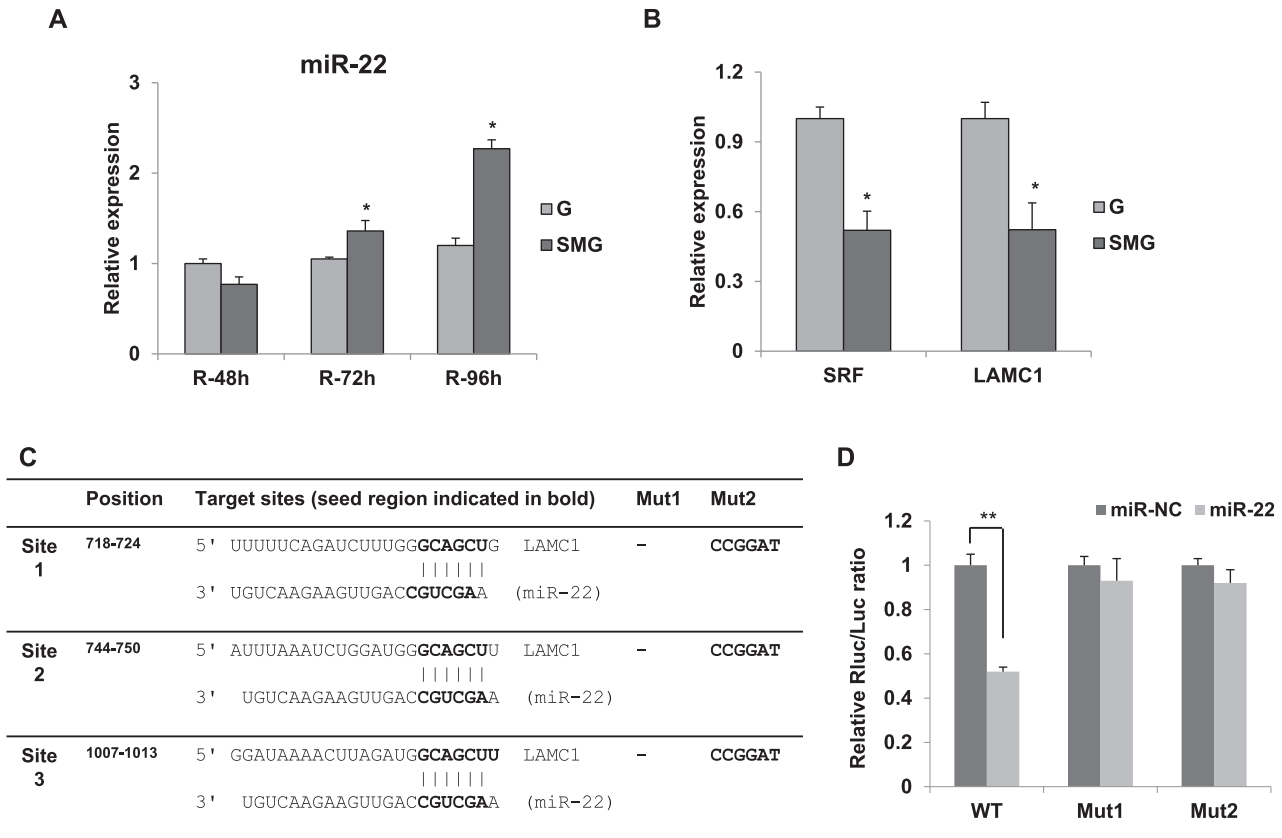


**Fig. 3.** The subsequent effect of SMG on expression levels of miR-22 and its target genes in HUVECs. A: Relative expression level of miR-22 was shown in SMG group compared to G group. B: SRF and LAMC1 at mRNA levels were quantified by qRT-PCR analysis in SMG group compared to G group at 72 h after return to normal gravity. \* $p < 0.05$  vs G. C: The 3'-UTR fragments of human SRF mRNA contain three putative miR-22 binding sites and mutant sequence (CGTCGA) was designed. D: pmiR-SRF-WT or pmiR-SRF-Mut was cotransfected with miR-22 mimics or miR-NC for 48 h. Luciferase activity was presented by relative hRlu/hLuc ratio. \*\* $p < 0.01$  vs miR-NC.

showed that miR-22 was up-regulated in a time-dependent manner (Fig. 3A) during subsequent culturing after SMG treatment. Therefore, we used a consensus approach with three widely used softwares (miRanda, Targetscan, PicTar) to perform target prediction. We wonder if SRF and LAMC1 might be involved in the alteration of HUVECs during subsequent culturing after SMG treatment. SRF and LAMC1 at mRNA expression levels were significantly down-regulated (Fig. 3B) in SMG group compared to G group at 72 h of subculture after SMG.

We predicted that the 3'-UTR fragments of human SRF mRNA contain three putative miR-22 binding sites (Fig. 3C) and luciferase reporter assay confirmed that SRF was the direct target for miR-22 (Fig. 3D). Further, we found that SRF siRNAs significantly resulted in cell growth inhibition and apoptosis (Fig. 4) in our previous study.<sup>27</sup> In the present study, we constructed pmiR-LAMC1-WT containing the complementary seed sequence of miR-22, pmiR-LAMC1-Mut1 (deletion of seed region) and pmiR-LAMC1-Mut2 (base substitution in seed region) at the 3'-UTR region of LAMC1 (Fig. 5A). The results showed that miR-22 significantly reduced the luciferase activities of pmiR-LAMC1-WT, compared with the miR negative control (miR-NC). In contrast, luciferase activities of two mutant reporters were not repressed by cotransfection with miR-22, implicating that LAMC1 is another direct target for miR-22 (Fig. 5B). Transfection of LAMC1 siRNAs (si-1, 2, 3) reduced LAMC1 protein expression (Fig. 6A) and significantly decreased cell adhesion rate (si-2:  $p < 0.01$ , si-3:  $P < 0.05$  in Fig. 6B). Downregulation of LAMC1 could inhibit the formation of actin stress fibers, but did not affect the localization of FAK in LAMC1 siRNA-transfected HUVECs (si-1: Fig. 6C).

## Discussion

A number of evidence show that microgravity can affect the structure and function in a variety of human and animal cells by the use of clinorotation-based systems.<sup>7,24,25,28</sup> RCCS-1 bioreactor represents a reasonable alternative to spaceflight and allows the modelling of microgravity on the ground. In the present study, we utilized RCCS-1 bioreactor to investigate cellular changes during subsequent culturing after SMG treatment. We here reported that when those SMG-treated cells returned to normal gravity, they displayed obvious growth inhibition, a transition from the decrease in cell adhesion ability in earlier time, actin cytoskeleton lesions within 72 h to induction of apoptosis in the later time. The mechanism of growth inhibition might be associated with miR-22 and mTOR/Apaf-1 signaling.

The effects of spaceflight on cardiovascular health after astronauts have returned should not be ignored because it is very important to understand the development of atherosclerosis and potential cardiovascular problems. Spaceflight leads to an internal environment that decreases plasma volume during flight but rebounds after flight, leading to a dilution of circulating soluble adhesion markers sICAM-1 and sE-selection.<sup>29</sup> Spaceflight-induced IL-6 and ICAM-1 remain to be elevated even after 3 months post spaceflight travel. The downregulation of eNOS expression in revived HUVEC cells suggests a reduced protection of the cells and the surrounding vessels against future insults that may lead to atherosclerosis.<sup>30</sup> Therefore, microgravity-induced endothelial dysfunction might occur after spaceflight or SMG treatment.

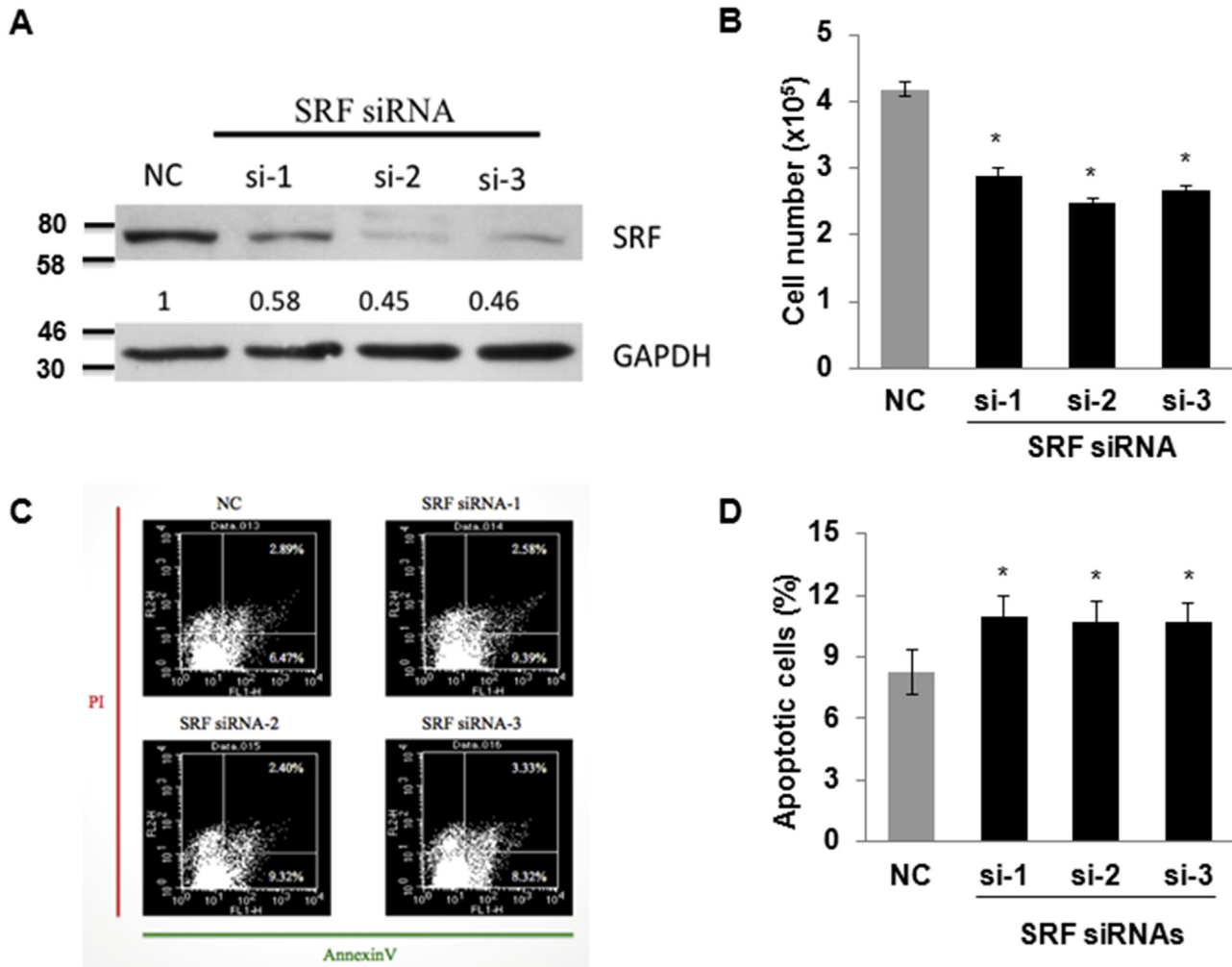


**Fig. 4.** The effects of SRF siRNAs on cell growth and apoptosis in HUVECs. A: The expression level of SRF protein was examined by western blot analysis. B: Cell numbers were counted in different groups. C: Early and later apoptotic rates were shown representative histograms. D: Percentage of total apoptotic cells was presented in different groups. \* $p < 0.05$  vs NC siRNA.

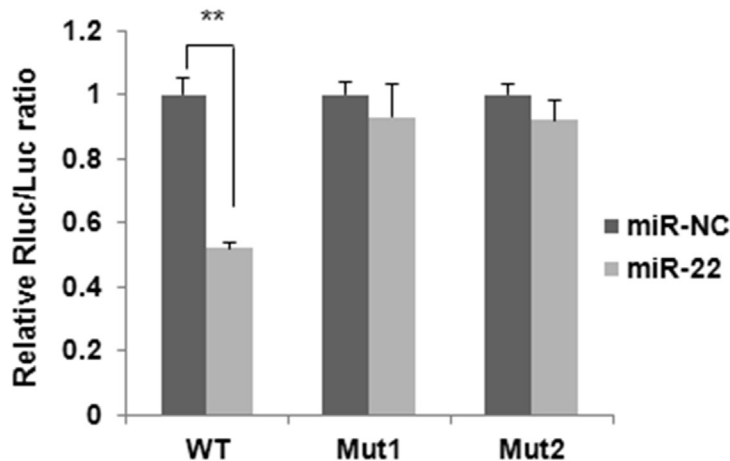
Exposure to microgravity generates alterations that are similar to those involved in age-related diseases, such as cardiovascular deconditioning, bone loss and muscle atrophy. Endothelial dysfunction is the common denominator,<sup>15</sup> which has been linked to human cardiovascular system disorders in spaceflight and post-spaceflight period. Revived HUVEC after real spaceflight exhibited persisting cytoskeletal changes and decreased cell growth indicating cellular senescence.<sup>16</sup> In the present study, we discovered a set of cellular responses in HUVECs after SMG treatment, including the decrease in cell adhesion ability in the earlier time, actin cytoskeleton lesions within 72 h, and induction of apoptosis in the later time. We found that cell adhesion ability decreased at 2 h and 4 h of subculture in the earlier time after SMG (Fig. 1B), implying that initial cells attached to the surface of culture dish in SMG group were less than that in G group. Cell adhesion rate recovered at 6 h of subculture might be attributed to the increasing cell number in the two groups. Cell adhesion can be involved in signal transduction and integrating cytoskeletal dynamics and cellular tension.<sup>31</sup> Endothelial cells have actin stress fibers, and the ends of stress fibers terminate at a structure similar to the adhesion plaque of cultured cells. The decrease in cell adhesion ability was observed in the earlier time after SMG, which might

trigger cellular signaling through adhesion plaque to affect endothelial cell structure and growth. Cytoskeletal structure is very critical for control of growth and cell fate switching.<sup>32</sup> We found that actin stress fiber formation was remarkably reduced at 24, 48 and 72 h of subculture after SMG (Fig. 1C), which was consistent with persisting cytoskeletal changes observed after real spaceflight.<sup>16</sup> Above all, we suppose that these alterations might commonly contribute to growth inhibition of human endothelial cells after SMG treatment.

Several studies showed transcription alterations in the endothelial cells exposed to microgravity. For example, PCNA transcript, a marker of cell mitosis, was found to be decreased in the absence of gravity.<sup>33</sup> Post-flight microarray analysis revealed 1023 significantly modulated genes, the majority of which are involved in cell adhesion, oxidative phosphorylation, stress responses, cell cycle, and apoptosis.<sup>15</sup> We suppose that those genes might be involved in growth inhibition of HUVECs after SMG treatment. In our study, we found the alterations of transcription factors SRF and mTOR, which are critical regulators in vascular endothelial cells and associated with endothelial dysfunction. Recent study has demonstrated SRF was a physiological target of miR-320a, implicated in cardiovascular diseases.<sup>17</sup> We also identified SRF as a novel target of miR-22

**A**

	Position	Target sites (seed region indicated in bold)	Mut1	Mut2
<b>Site 1</b>	718-724	5' UUUUUCAGAUUUUGGG <b>CAGCUG</b> LAMC1	-	CCGGAT
		3' UGUCAAGAAGUUGACCGUCGAA (miR-22)		
<b>Site 2</b>	744-750	5' AUUUAAAUCUGGAUGGG <b>CAGCUU</b> LAMC1	-	CCGGAT
		3' UGUCAAGAAGUUGACCGUCGAA (miR-22)		
<b>Site 3</b>	1007-1013	5' GGAUAAAACUAGAUG <b>GCAGCUU</b> LAMC1	-	CCGGAT
		3' UGUCAAGAAGUUGACCGUCGAA (miR-22)		

**B**

**Fig. 5.** LAMC1 is a direct target of miR-22. A: The 3'-UTR fragments of human LAMC1 mRNA contain three putative miR-22 binding sites. Mut1 is deletion of seed region and Mut2 is base substitution in seed region. B: pmir-LAMC1-WT or pmir-LAMC1-Mut1/2 was cotransfected with miR-22 mimics or miR-NC for 48 h. Luciferase activity was presented by relative hRlu/hluc ratio. \*\* $p < 0.01$  vs miR-NC.

and found that miR-22 caused apoptosis and inflammation in HUVECs via targeting SRF.<sup>27</sup> Here, we demonstrated that miR-22 was up-regulated but SRF was down-regulated in SMG group compared to G group after SMG, indicating that SRF might be involved in growth inhibition and apoptosis during subsequent culturing after SMG treatment. It is reported that LAMC1 is important for bodies to keep stability and control growth.<sup>34</sup> We found that LAMC1 could regulate cell proliferation and cytoskeleton changes through FAK signaling in endosulfan-exposed cells.<sup>23</sup> Here, we confirmed LAMC1 is a novel target gene of miR-22. LAMC1 siRNAs (si-2, 3) significantly decreased cell adhesion rate and each LAMC1 siRNA disrupted the formation of stress fibers. LAMC1 was down-regulated in SMG group compared to G group after SMG, indicating that LAMC1 might be associated with the alteration of cell adhesion and actin cytoskeleton during subsequent culturing after SMG treatment. In addition, a mammalian counterpart of TOR complex 2 (mTORC2) contains mTOR and seems to function upstream of Rho GTPases to regulate the actin cytoskeleton.<sup>35</sup> It is possible that the alteration of actin

cytoskeleton was associated with mTORC2, which needs to be further discussed.

It was previously demonstrated that miR-22 reduces the expression of PTEN, a negative regulator of the AKT pathway in cardiomyocytes.<sup>36</sup> miR-22 may suppress autophagy through activation of AKT, which may, in turn, activate the kinase mTOR, a negative regulator of the autophagic process.<sup>37</sup> In this study, PTEN was not down-regulated by miR-22. In fact, we observed the mild increase in PTEN protein expression levels during subsequent culturing after SMG treatment (data not shown). It is reported that PTEN could inhibit the proliferation and promote apoptosis of K562 cells through regulating mTOR signaling pathway.<sup>19</sup> Expression of mTOR and its downstream Apaf-1 were remarkably up-regulated in SMG group compared to G group. Therefore, the mechanism of growth inhibition after SMG treatment may be explained by alterations of mTOR signaling and miR-22-mediated mechanism.

In conclusion, the evidence presented the subsequent effects of SMG on HUVECs and mainly involves examination of the underlying mechanisms of growth inhibition during subsequent

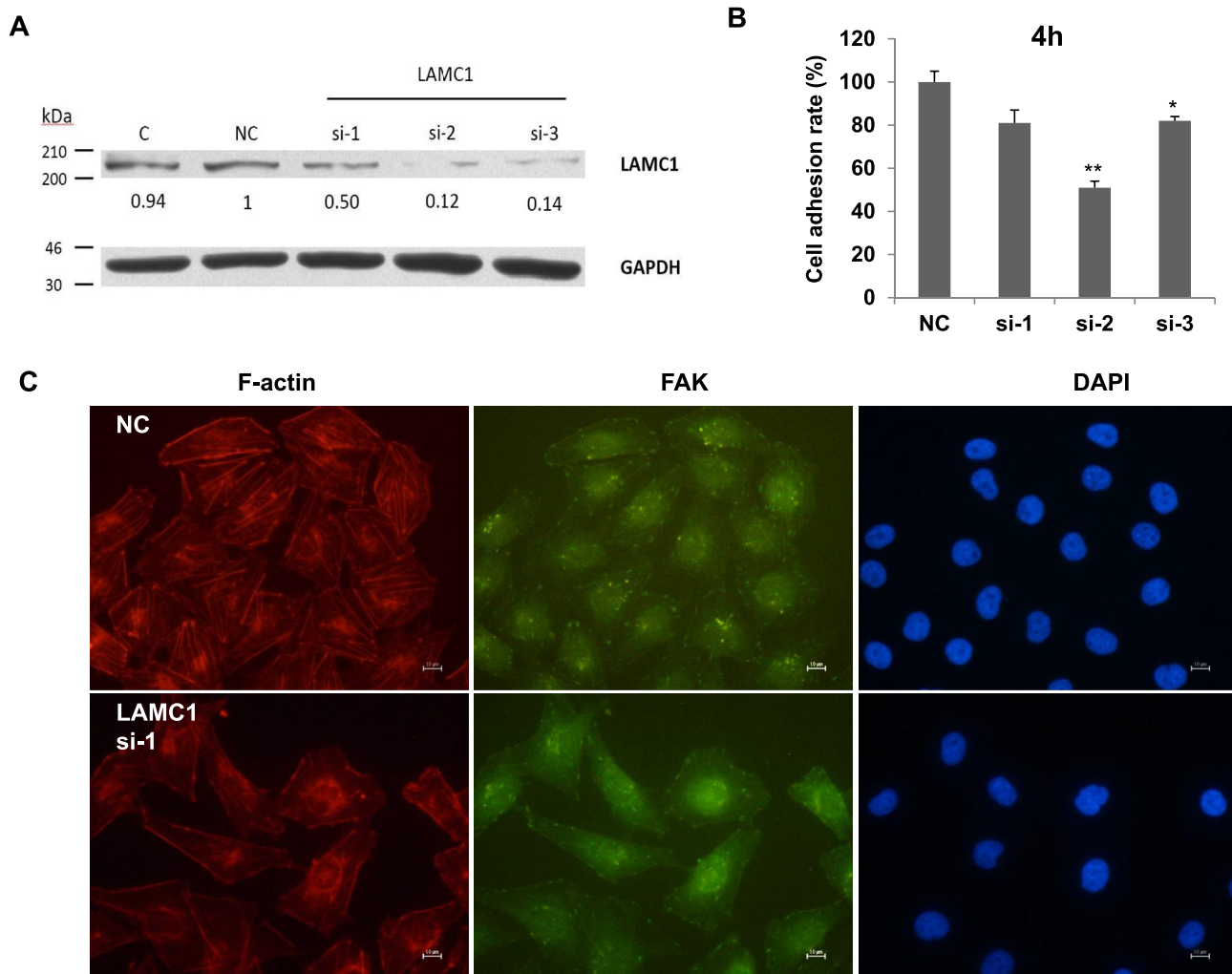


**Fig. 6.** The effects of LAMC1 siRNAs on cell adhesion and actin cytoskeleton in HUVECs. A: The expression level of LAMC1 protein was examined by western blot analysis. B: Cell adhesion rate were analyzed in different groups at 4h after subculture. C: HUVECs were stained with the Rhodamine-conjugated phalloidin (red) and FAK (green) at 48 h after transfection with NC siRNA or LAMC1 si-1. The representative images show alteration of actin cytoskeleton. Scale bar, 25  $\mu\text{m}$  \* $p < 0.05$ , \*\* $p < 0.01$  vs NC siRNA.

culturing after SMG treatment. Our data presented here open a wide range of specific investigations in terms of subsequent effects of microgravity, providing a better understanding of the underlying mechanisms in biological processes of the cardiovascular systems after microgravity.

## Fund

This study was supported by the "National Natural Science Foundation of China (No. 31270903)" and the Fundamental Research Funds for the Central Universities (3132016330).

## References

- White RJ, Averner M. Humans in space. *Nature*. 2001;409:1115–1118.
- Hatton DC, Yue Q, Dierickx J, et al. Calcium metabolism and cardiovascular function after spaceflight. *J Appl Physiol*. 1985;2002(92):3–12.
- Riwaldt S, Bauer J, Pietsch J, et al. The importance of caveolin-1 as key-regulator of three-dimensional growth in thyroid cancer cells cultured under real and simulated microgravity conditions. *Int J Mol Sci*. 2015;16:28296–28310.
- Uva BM, Masini MA, Sturla M, et al. Clinorotation-induced weightlessness influences the cytoskeleton of glial cells in culture. *Brain Res*. 2002;934:132–139.
- Schatten H, Lewis ML, Chakrabarti A. Spaceflight and clinorotation cause cytoskeleton and mitochondria changes and increases in apoptosis in cultured cells. *Acta Astronaut*. 2001;49:399–418.
- Blaber EA, Dvorochkin N, Lee C, et al. Microgravity induces pelvic bone loss through osteoclastic activity, osteocytic osteolysis, and osteoblastic cell cycle inhibition by CDKN1a/p21. *PLoS One*. 2013;8:e61372.
- Masiello MG, Cucina A, Proietti S, et al. Phenotypic switch induced by simulated microgravity on MDA-MB-231 breast cancer cells. *BioMed Res Int*. 2014;2014:652434.
- Coinu R, Chiaviello A, Galleri G, et al. Exposure to modeled microgravity induces metabolic idleness in malignant human MCF-7 and normal murine VSMC cells. *FEBS Lett*. 2006;580:2465–2470.
- Makihira S, Kawahara Y, Yuge L, et al. Impact of the microgravity environment in a 3-dimensional clinostat on osteoblast- and osteoclast-like cells. *Cell Biol Int*. 2008;32:1176–1181.
- Endemann DH, Schiffrin EL. Endothelial dysfunction. *J Am Soc Nephrol*. 2004;15:1983–1992.
- Maier JA, Cialdai F, Monici M, et al. The impact of microgravity and hypergravity on endothelial cells. *BioMed Res Int*. 2015;2015:434803.
- Versari S, Villa A, Bradamante S, et al. Alterations of the actin cytoskeleton and increased nitric oxide synthesis are common features in human primary endothelial cell response to changes in gravity. *Biochim Biophys Acta*. 2007;1773:1645–1652.
- Carlsson SI, Bertilaccio MT, Ballabio E, et al. Endothelial stress by gravitational unloading: effects on cell growth and cytoskeletal organization. *Biochim Biophys Acta*. 2003;1642:173–179.
- Infanger M, Kossmehl P, Shakibaei M, et al. Induction of three-dimensional assembly and increase in apoptosis of human endothelial cells by simulated



- microgravity: impact of vascular endothelial growth factor. *Apoptosis*. 2006;11:749–764.
15. Versari S, Longinotti G, Barenghi L, et al. The challenging environment on board the International Space Station affects endothelial cell function by triggering oxidative stress through thioredoxin interacting protein overexpression: the ESA-SPHINX experiment. *FASEB J*. 2013;27:4466–4475.
  16. Kapitonova MY, Muid S, Froemming GR, et al. Real space flight travel is associated with ultrastructural changes, cytoskeletal disruption and premature senescence of HUVEC. *Malays J Pathol*. 2012;34:103–113.
  17. Chen C, Wang Y, Yang S, et al. MiR-320a contributes to atherogenesis by augmenting multiple risk factors and down-regulating SRF. *J Cell Mol Med*. 2015;19(5):970–985.
  18. Weichhart T. Mammalian target of rapamycin: a signaling kinase for every aspect of cellular life. *Methods Mol Biol*. 2012;821:1–14.
  19. Cheng ZY, Guo XL, Yang XY, et al. PTEN and rapamycin inhibiting the growth of K562 cells through regulating mTOR signaling pathway. *J Exp Clin Cancer Res*. 2008;27:87.
  20. Shang YC, Chong ZZ, Wang S, et al. Erythropoietin and Wnt1 govern pathways of mTOR, Apaf-1, and XIAP in inflammatory microglia. *Curr Neurovascular Res*. 2011;8:270–285.
  21. Peng N, Meng N, Wang S, et al. An activator of mTOR inhibits oxLDL-induced autophagy and apoptosis in vascular endothelial cells and restricts atherosclerosis in apolipoprotein E(-)/(-) mice. *Sci Rep*. 2014;4:5519.
  22. Tzu J, Marinkovich MP. Bridging structure with function: structural, regulatory, and developmental role of laminins. *Int J Biochem Cell Biol*. 2008;40:199–214.
  23. Xu D, Liu T, Lin L, et al. Exposure to endosulfan increases endothelial permeability by transcellular and paracellular pathways in relation to cardiovascular diseases. *Environ Pollut*. 2017;223:111–119.
  24. Meyers VE, Zayzafoon M, Douglas JT, et al. RhoA and cytoskeletal disruption mediate reduced osteoblastogenesis and enhanced adipogenesis of human mesenchymal stem cells in modeled microgravity. *J Bone Miner Res*. 2005;20:1858–1866.
  25. Wang Y, An L, Jiang Y, et al. Effects of simulated microgravity on embryonic stem cells. *PLoS One*. 2011;6:e29214.
  26. Siamwala JH, Reddy SH, Majumder S, et al. Simulated microgravity perturbs actin polymerization to promote nitric oxide-associated migration in human immortalized Eahy926 cells. *Protoplasma*. 2010;242:3–12.
  27. Dan X, Guo Y, Tong L, et al. miR-22 contributes to endosulfan-induced endothelial dysfunction by targeting SRF in HUVECs. *Toxicol Lett*. 2017;269:33–40.
  28. Morabito C, Steimberg N, Mazzoleni G, et al. RCCS bioreactor-based modelled microgravity induces significant changes on in vitro 3D neuroglial cell cultures. *BioMed Res Int*. 2015;2015:754283.
  29. Austin AW, Patterson SM, Ziegler MG, et al. Plasma volume and flight duration effects on post-spaceflight soluble adhesion molecules. *Aviat Space Environ Med*. 2014;85:912–918.
  30. Muid S, Froemming GR, Ali AM, et al. Interleukin-6 and intercellular cell adhesion molecule-1 expression remains elevated in revived live endothelial cells following spaceflight. *Malays J Pathol*. 2013;35:165–176.
  31. Parsons JT, Horwitz AR, Schwartz MA. Cell adhesion: integrating cytoskeletal dynamics and cellular tension. *Nature Rev Mol Cell Biol*. 2010;11:633–643.
  32. Mammoto A, Ingber DE. Cytoskeletal control of growth and cell fate switching. *Curr Opin Cell Biol*. 2009;21:864–870.
  33. Morbidelli L, Monici M, Marziliano N, et al. Simulated hypogravity impairs the angiogenic response of endothelium by up-regulating apoptotic signals. *Biochem Biophys Res Commun*. 2005;334:491–499.
  34. Yang DH, Mckee KK, Chen ZL, et al. Renal collecting system growth and function depend upon embryonic  $\gamma$ 1 laminin expression. *Development*. 2011;138:4535–4544.
  35. Jacinto E, Loewith R, Schmidt A, et al. Mammalian TOR complex 2 controls the actin cytoskeleton and is rapamycin insensitive. *Nature Cell Biol*. 2004;6:1122–1128.
  36. Xu XD, Song XW, Li Q, et al. Attenuation of MicroRNA-22 derepressed PTEN to effectively protect rat cardiomyocytes from hypertrophy. *J Cell Physiol*. 2012;227:1391–1398.
  37. Sciarretta S, Volpe M, Sadoshima J. Mammalian target of rapamycin signaling in cardiac physiology and disease. *Circ Res*. 2014;114:549.